ACS APPLIED MATERIALS & INTERFACES

RESEARCH ARTICLE

www.acsami.org

Phthalimido-boronsubphthalocyanines: New Derivatives of Boronsubphthalocyanine with Bipolar Electrochemistry and Functionality in OLEDs.

Graham E. Morse,[†] Jeffery S. Castrucci,[†,‡] Michael G. Helander,[‡] Zheng-Hong Lu,[‡,⊥] and Timothy P. Bender*[,†,‡,§]

[†]Department of Chemical Engineering and Applied Chemistry, University of Toronto, 200 College Street, Toronto, Ontario, Canada M5S 3E5

[‡]Department of Materials Science and Engineering, University of Toronto, 184 College Street, Toronto, Ontario, Canada M5S 3E4

[§]Department of Chemistry, University of Toronto, 80 St. George Street, Toronto, Ontario, Canada M5S 3H6

[⊥]Department of Physics, Yunnan University, 2 Cuihu Beilu, Yunnan, Kunming 650091, People's Republic of China.

Supporting Information

ABSTRACT: Phthalimides have been found to react with Cl-**BsubPc** to produce a new class of **BsubPc** derivatives, phthalimido-boronsubphthalocyanines (Phth-**BsubPc**s). They exhibit a high quantum yield for photoluminescence (Φ), maintain a high molar extinction coefficient (ε) and have bipolar electrochemical stability previously unseen in simple **BsubPc** derivatives. Their bipolar electrochemical characteristics have been extended into simple organic electronic devices: in OLEDs as charge transporters and emitters.

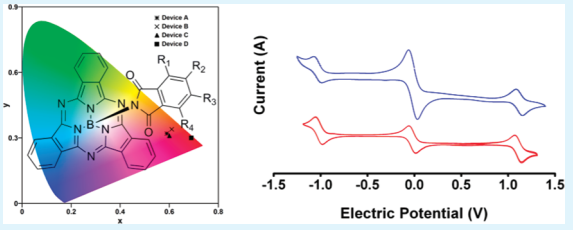

KEYWORDS: boron, subphthalocyanine, phthalimide, bipolar, organic, electronics, schottky junction, solar cell, light emitting diode

INTRODUCTION

While chloroboronsubphthalocyanine (Cl-**BsubPc**) was discovered in 1972,[1] **BsubPc** derivatives have only recently emerged as functional materials in a variety of applications including: organic electronic devices such as photovoltaic cells (OPVs),[2] chemical sensors,[3] light-emitting diodes (OLEDs),[4] and thin film transistors (OTFTs);[5] supramolecular building blocks for molecular cages;[6] molecular sensors for recognition of large molecules such as fullerene[7] and porphyrins;[8] and biological systems as photosensitizers for photodynamic therapy[9] and as testosterone marker-tags.[10] The **BsubPc** derivatives which are most commonly employed are either a halo-**BsubPc** (commonly a chloride) or a derivative thereof whereby the halide has been displaced with a nucleophile thus placing an additional molecular fragment in the axial position of the **BsubPc**. Displacement of the halide of halo-**BsubPc**s has conventionally been limited to reaction with oxygen- (phenols,[11,12a] alcohols,[12] water,[13] and silanols[14]) and carbon (Grignards[15])-based nucleophiles.

During the course of our research we have discovered that phthalimides can also function as suitable nucleophiles and displace the chloride of Cl-**BsubPc** to form phthalimido-boronsubphthalocyanines (Phth-**BsubPc**, Scheme 1). This is done without the aid of expensive catalysts or reagents. Concurrent with our study Guilleme et al. have highlighted the need to expand to other nucleophiles for the formation of novel derivatives of **BsubPc**s and have put forward an approach to accessing alternative nucleophiles. Their approach utilizes silver triflate as a halophilic reagent which extracts the chloride from Cl-**BsubPc** to generate TfO-**BsubPc** in situ. Exposure to nucleophilic reagents results in the formation of the desired **BsubPc** derivative.[16]

We wish to additionally report that Phth-**BsubPc**s have a previously unseen crystallographic arrangement and unique photophysical, electrochemical, and electronic properties when compared with existing **BsubPc** derivatives, which can be attributed to the phthalimido molecular fragment. This includes bipolar electrochemical behavior.

RESULTS AND DISCUSSION

Phth-**BsubPc**s were easily synthesized using conditions similar to those used for reaction of Cl-**BsubPc** with phenol.[11] Specifically, five equivalents of phthalimide or tetrachlorophthalimide were reacted with Cl-**BsubPc** (**1**) initially in refluxing chlorobenzene to form phthalimido-**BsubPc** (Phth-**BsubPc**, compound **2**) and tetrachlorophthalimido-**BsubPc** (Cl_4Phth-**BsubPc**, compound **3**) respectively (Scheme 1). Under these conditions we noticed that conversion was nearly quantitative but excessively slow. We therefore repeated the reactions in refluxing dichlorobenzene, which at elevated temperature achieved ~90%

Received: June 13, 2011
Accepted: August 3, 2011
Published: August 03, 2011

Scheme 1. Reaction of Cl-BsubPc (1) with Phthalimide or Tetrachlorophtalimide to Give Phth-BsubPcs 2 and 3 (respectively)[a]

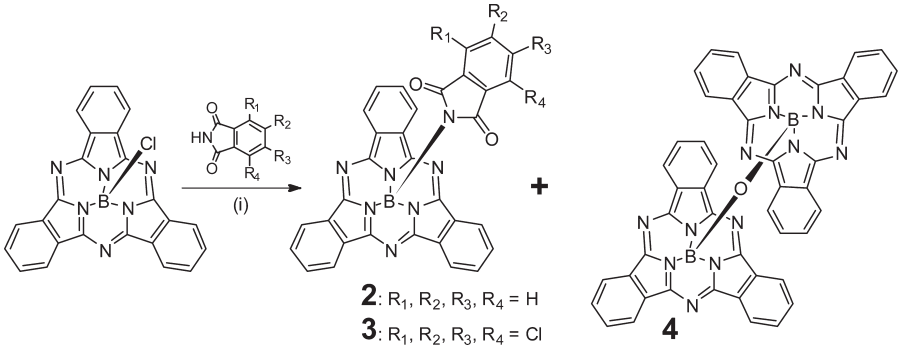

[a] Conditions: (i) 5 equiv, 1,2-dichlorobenzene or chlorobenzene, reflux.

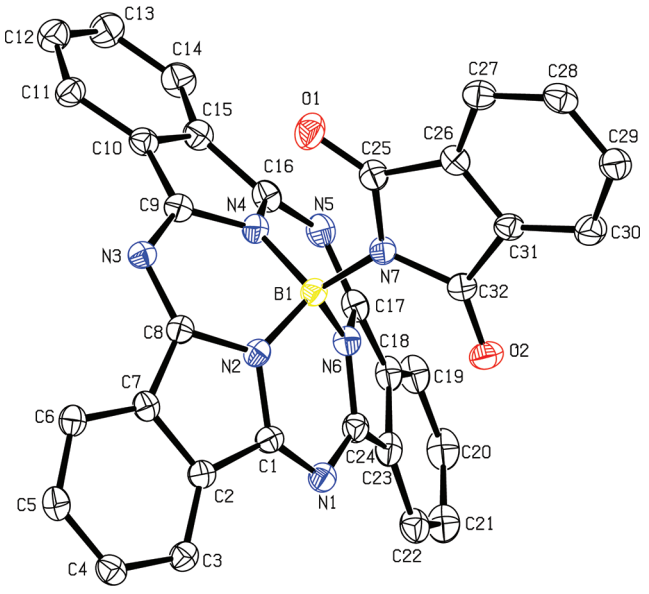

Figure 1. Thermal ellipsoid plot of **2** showing 35% probability. Hydrogen atoms have been omitted for clarity.

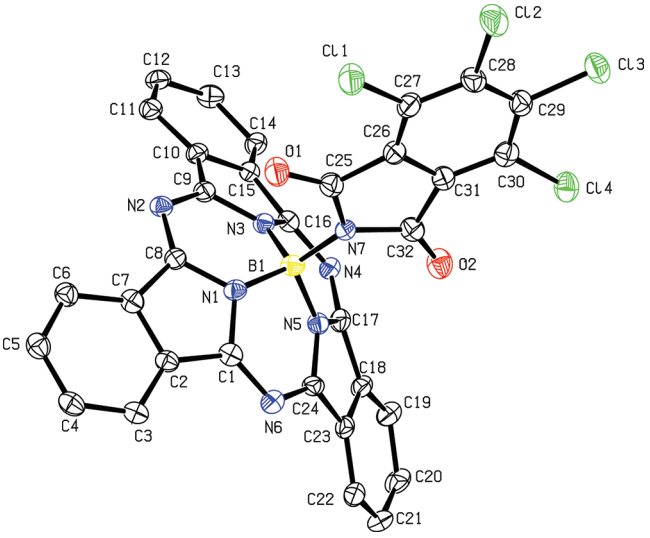

Figure 2. Thermal ellipsoid plot of **3** showing 35% probability. Hydrogen atoms have been omitted for clarity.

conversion to the respective Phth-**BsubPc** in 100 h for phthalimide and 90 h for tetrachlorophthalimide.[17] The formation of a byproduct of ~10% (by HPLC) was identified as μ-oxo-(**BsubPc**)$_2$ (**4**, confirmed by HRMS and UV−vis spectroscopy, see the Supporting Information). μ-Oxo-(**BsubPc**)$_2$ is presumably formed when trace amounts of water present in the reaction vessel (either initially or over the 100 h reaction time) hydrolyze Cl-**BsubPc** to HO-**BsubPc**, which subsequently undergoes self-condensation or reaction with another equivalent of Cl-**BsubPc**.[13,14b,18] Surprisingly, use of the potassium salt of phthalimide at the same temperature in either dichlorobenzene or dimethylformamide (or mixtures thereof) did not yield **2**. Attempts to react Cl-**BsubPc** with 1,8-naphthalimide were unsuccessful. Finally, we also attempt reaction of aniline, *N*-methylaniline, and diphenylamine under similar conditions. No conversion to product was observed.

Purification of Phth-**BsubPc**s was achieved by train sublimation of the crude product. The Phth-**BsubPc**s were collected as the slowest moving golden/bronze band deposited as a crystalline film. Whereas μ-oxo-(**BsubPc**)$_2$ does not sublime under these conditions. The deposited band of Phth-**BsubPcs** in each case contained single crystals suitable for X-ray diffraction. In each case the molecular structure of the Phth-**BsubPc**s was confirmed (Figure 1 and 2). The orientation of the phthalimido molecular fragment relative to the **BsubPc** fragment is nearly perpendicular, which is similar to that obtained when carbon-based nucleophiles are used[15] while being very different from that seen for phenoxy derivatives.[11,12a] Single crystals were also grown by slow diffusion of heptane into a solution of each Phth-**BsubPc** in chloroform. Compound **3** had an identical crystal structure by this method to that obtained by train sublimation while compound **2** included solvent in its crystal under these conditions (see the Supporting Information).

With regards to photophysical properties, both **2** and **3** possess a UV−visible absorption profile characteristic of **BsubPc** derivatives. Their absorption maxima are slightly shifted bathochromically compared to compound **1** at 565 to 569 nm ($\varepsilon = 6.9 \times 10^4\,L\,M^{-1}cm^{-1}$) and 571 nm ($\varepsilon = 6.4 \times 10^4\,L\,M^{-1}cm^{-1}$) respectively (Figure 3).[14b] Optical band gaps of 2.13 and 2.12 eV were calculated from the onset of the longest wavelength absorption peak (from their solution spectra).[5a,2c] Upon photoexcitation, luminescence with a very small Stokes shift of was

observed (in toluene of 8 nm for **2** and 9 nm for **3**) resulting in emission maxima at 577 and 579 nm respectively (Figure 3). Solution-state quantum yields (Φ) were measured using phenoxy-dodecafluoroboronsubphthalocyanine ($\mathbf{F_{12}BubPc}$) as a reference compound (which has been previously reported[15,3a] and verified by our group). We found the quantum efficiencies to be 0.40 and 0.47 for **2** and **3**, respectively, which is similar to that determined for other **BsubPc** derivatives.[19] Solid-state absorption and photoluminescence spectra were measured on ~35 nm thick films deposited by sublimation onto a quartz substrate. The solid-state absorption maxima are each bathochromically shifted from their solution measurements by 18 to 587 nm (ε = 60 000 L mol^{-1} cm^{-1}) and 588 nm (ε = 53 000 L mol^{-1} cm^{-1}) for **2** and **3**, respectively. Unlike our liquid state measurements, the solid-state photoluminescence spectrum had four emission peaks for compound **2** (602, 657, 729, and 820 nm) and compound **3** (603 nm, 649 nm, 720 nm, 820 nm). Because the solution-state photoluminescence is normally behaved and consistent in profile with other **BsubPc**s (Figure 3), we must conclude this complex emission in the solid state is not a function of the molecular structure rather it is a result of the arrangement of **2** and **3** in the solid state. We are currently in the process of investigating the root cause of the complex solid state emission.

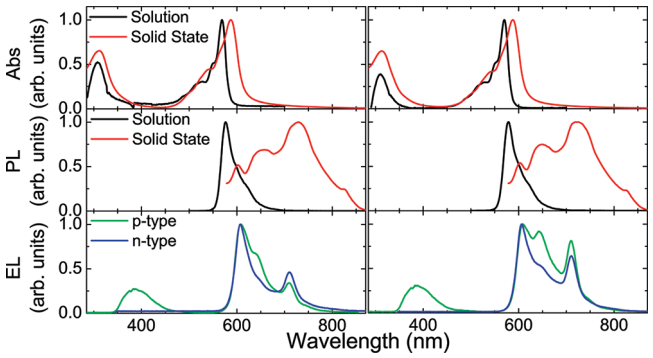

Figure 3. Normalized absorption (Abs), photoluminescence (PL), and electroluminescence (EL) spectra of compounds **2** (left) and **3** (right). Solution denotes spectra that were measured from dilute (3×10^{-7} mol L^{-1}) toluene solutions, while solid state denotes spectra measured from thin (100 nm) films made by physical vapor deposition on quartz substrates. All PL spectra were collected using an excitation wavelength of 480 nm. p-Type denotes OLED structures were compounds **2** or **3** are used as a hole transport and emission layer (ITO/ **2** or **3** (50 nm)/TPBi (50 nm)/LiF (3 nm)/Al (100 nm)) and n-type denotes OLED structures were compounds **2** or **3** are used as an electron transport and emission layer (ITO/NPB (50 nm)/**2** or **3** (50 nm)/TPBi (3 nm)/Al (100 nm)). p-Type EL spectra are shown at a driving voltage of 9 V while n-type EL spectra are shown at a driving voltage of 5 V.

Anthony has shown that organic materials that order in extended π-stacked arrays in the solid state exhibit high charge mobilities in organic electronic devices.[20] It has also been shown that the electronic coupling of molecules, leading to high charge carrier mobilities, increases with increasing frontier molecular orbital overlap in the solid state.[21] Phenoxy-**BsubPc**s, within their extended solid state arrangement, commonly order in a concave−concave head-to-head π-interaction resulting in the formation of a repeating dimeric motif throughout the crystal.[22,4a,23] This motif however lacks π-interactions between the dimers throughout the bulk of the crystal.[21a] In contrast, we and others have shown that phenoxy-dodecafluoro**BsubPcs** tend to arrange in extended π-stacked arrays along a crystallographic axis.[4a,24] The solid-state packing for Phth-**BsubPc**s **2** and **3** are distinctly different from either of these commonly observed arrangements. The packing of **2** is such that the **BsubPc** molecular fragments π-stack in a concave−concave head-to-head fashion with a neighboring **BsubPc** each overlapping one of their isoindoline units at a distance of 3.7744(16) Å (centroid of C18/C19/C20/C21/C22/C23 to centroid of N6/C17/C18/C23/C24, see Figure S1 in the Supporting Information and atomic numbering in Figure 1). An additional interaction is observed between pairs of axial phthalimide molecular fragments which π-stack at a ring centroid distance of 3.7816(18) Å (from C26/C27/C28/C29/C30/C31 to N7/C25/C26/C31/C32, see Figure S2 in the Supporting Information). The sum of these interactions produces channel volumes of exclusively **BsubPc** fragments and others of exclusively phthalimide fragments orientated along the crystallographic *c*-axis (Figure 4). This arrangement is similar to that observed in the solid-state arrangement of ethynyl-**BsubPcs**[15a] and thiophenylphenoxy-**BsubPcs**.[15b] Within the solid-state arrangement of **3**, the intramolecular arrangement is entirely different, whereby a concave-to-ligand interaction between the six-membered ring of the tetrachlorophthalimide fragment (C26/C27/C28/C29/C30/C31) and a six-membered ring of the **BsubPc** molecular fragment (C2/C3/C4/C5/C6/C7) occurs at a centroid to centroid distance of 3.594(3) Å

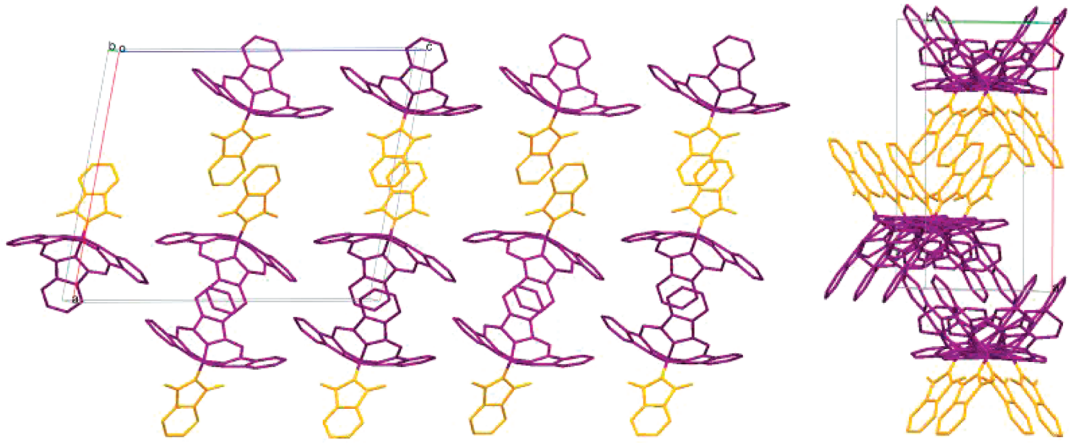

Figure 4. Section of the unit cell of Phth-**BsubPc 2** viewed along the *b* (left) and *c* (right) axis showing the $\pi-\pi$ extended stacking pathways. The **BsubPc** and phthalimide segments have been colored purple and yellow, respectively.

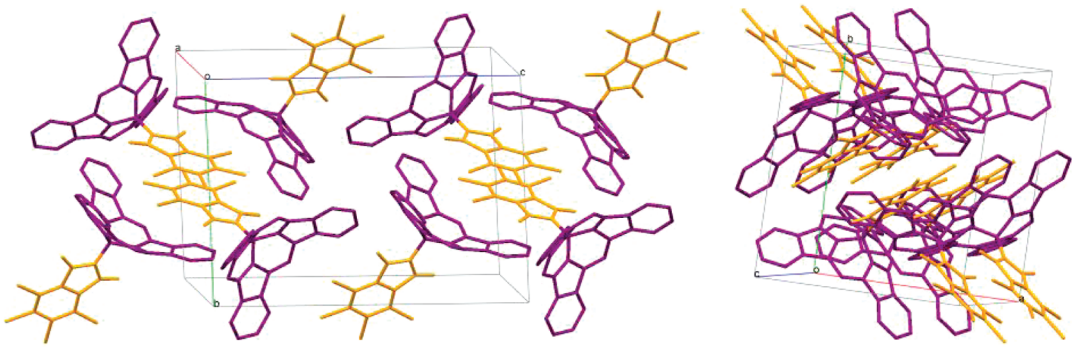

Figure 5. A section of the unit cell of Phth-**BsubPc 3** facing the *bc* plane (left) and *ac* plane (right) showing the $\pi-\pi$ extended stacking pathways. The **BsubPc** and phthalimide segments have been colored purple and yellow, respectively.

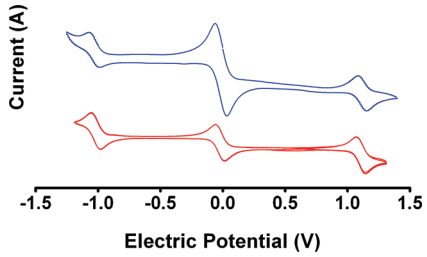

Figure 6. Cyclic voltammagrams of compounds **2** (blue) and **3** (red) in dichloromethane with tetrabutylammonium hexafluorophosphate (Bu_4NPF_6) as electrolyte. The wave near zero volts is that of decamethylferrocene, which was used as an internal standard and referenced to −0.012 V.

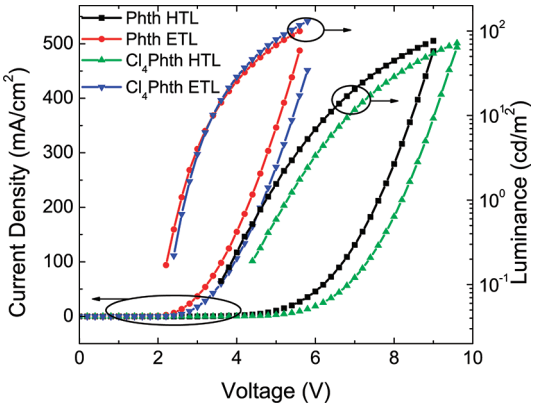

Figure 7. Luminance and current density as a function of voltage for OLED devices including **BsubPc** as an HTL and ETL. HTL devices architecture: ITO/**BsubPc** (50 nm)/TPBi (50 nm)/LiF (1 nm)/Al (100 nm); ETL devices architecture: ITO/NPB (50 nm)/**BsubPc** (50 nm)/TPBi (3 nm)/Al (100 nm).

(see Figure S3 in the Supporting Information). This arrangement is then mirrored to another pair of molecules and forms the repeating motif that extends throughout the structure forming continuous stair-like stacks (Figure 5). Modeling of the frontier orbitals of both **2** and **3** using density functional theory methods (6-31G* basis set) indicates the presence of electron density around both the **BsubPc** macrocycle and the axial phthalimide for the HOMO to HOMO-4 and the LUMO to LUMO+4 frontier orbitals (see Figure S4 in the Supporting Information). This is in contrast to the complete lack of orbital density on the phenoxy molecular fragment of phenoxy-**BsubPcs**.[25] Thus there is a potential for the HOMO and LUMO to permeate throughout the extended solid state arrangement in the exclusively **BsubPc** and/or exclusively phthalimido columns.

Prior to incorporation into electronic devices, we investigated the electrochemical behavior of **2** and **3** using standard cyclic voltammetry procedures across a range of potentials from +1600 mV to −1600 mV in dilute dichloromethane solution. Compounds **2** and **3** each exhibited reversible oxidation and reversible reduction events, with compound **2** having half-wave potentials at +1117 and −1009 mV and compound **3** having half-wave potentials at +1148 and −962 mV (vs Ag/AgCl, Figure 6). Using the equations developed by Forrest, Thompson, and colleagues,[26] the measured reduction and oxidation potentials predict a HOMO energy of 5.61 and 5.66 eV for **2** and **3**, respectively. By using the aforementioned optical bandgaps, a LUMO energy of 3.48 and 3.54 eV can be estimated. The reversible bipolar electrochemical behavior of **2** and **3** is in contrast to what is more commonly seen for **BsubPc** derivatives. Table S1 in the Supporting Information outlines a survey of the electrochemical behavior of a variety of **BsubPc** derivatives reported in the literature. Overall, it shows phenoxy-**BsubPc** derivatives commonly oxidize irreversibly and reduce reversibly while a large portion of arylethynyl-**BsubPcs**[15] and alkoxy-**BsubPcs**[10f] show reversible oxidations and reductions. We have also reported the preference for pentafluorophenoxy-**BsubPc** (**F_5BsubPc**) to undergo reversible reduction and subsequently perform as an *n*-type material in an OLED.[4a]

An array of bilayer OLEDs were fabricated using each Phth-**BsubPc**, whereby each compound operated as a *p*-type carrier, or an *n*-type carrier and an emitter. We have previously demonstrated that fluorinated phenoxy-**BsubPcs** behave as *n*-type carriers and emitters.[4a] We first constructed devices of the following architecture (whereby compounds **2** and **3** would function in an electron transport layer (ETL) and as an emitter): ITO/NPB (50 nm)/**BsubPc** (50 nm)/LiF (1 nm)/Al (100 nm), where NPB (*N*,*N*′-bis(1-naphthyl)-*N*,*N*′-diphenyl-1,1′-biphenyl-4,4′-diamine) is a well-known[27] *p*-type transport material (see Figure S5 in the Supporting Information). Compound **2** performed well, with a turn on voltage of 2.8 V with a maximum efficiency of 0.01 cd/A (36 cd/m^2), whereas compound **3** performed significantly worse <0.01 cd/A (3 cd/m^2). To increase the charge current density in the *n*-type films, we explored

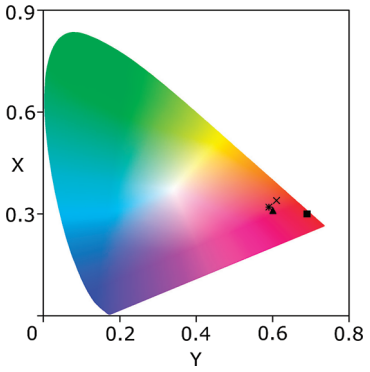

Figure 8. CIE color coordinates (symbol; *x*, *y*) for the light emission produced by the OLED devices. For HTL devices with compound **2** (□; 0.58, 0.32) and compound **3** (▲; 0.60, 0.32): ITO/**BsubPc** (50 nm)/TPBi (50 nm)/LiF (1 nm)/Al (100 nm); and for ETL devices with compound **2** (× ; 0.61, 0.34) and compound **3** (■; 0.69, 0.31): ITO/NPB (50 nm)/**BsubPc** (50 nm)/TPBi (3 nm)/Al (100 nm).

using 1,3,5-tris(N-phenyl-benzimidazole-2-yl)benzene (TPBi) as electron injection layer in place of LiF and found drastic increases in performance, reducing turn on voltages to 2.6 and 2.8 V, and increasing maximum efficiency to 0.02 cd/A (100 cd/m^2) and 0.03 cd/A (143 cd/m^2) for compounds **2** and **3** respectively (Figure 7). This performance is comparable to that of our previously reported pentafluorophenoxy-**BsubPc** (**F$_5$BsubPc**) within a similar architecture.[4a] Subsequently, we constructed devices with an architecture of ITO/**BsubPc** (50 nm)/TPBi (50 nm)/LiF (1 nm)/Al (100 nm) whereby compounds **2** and **3** were to function as a hole transport layer (HTL) and as an emitter (see Figure S5 in the Supporting Information). Compound **2** performed well, with a turn on voltage of 4.8 V with an efficiency of 0.02 cd/A (77 cd/m^2); compound **3** produced similar results (Figure 7, see Table S2 in the Supporting Information). The relatively high turn on voltages for these devices could be attributed to a combination of the HOMO−LUMO offset between TPBi and the **BsubPc**s (calculated to be ∼3 eV) or between NPB and the **BsubPc**s (calculated to be ∼2 eV), and poor charge injection (see Figure S6 in the Supporting Information). Interestingly with compounds **2** and **3** as the ETL, we found it to be largely alleviated by using TPBi in place of LiF, similar to our observations for fluorinated phenoxy-**BsubPc**s.[4a]

The electroluminescence (EL) from these devices displayed multiple emission peaks similar to their solid state PL (similar in peak location, but not their relative intensities). Three peaks at 607−609, 637−642, and 710 nm were observed when operating as a *p*-type or *n*-type emitter resulting in an orange-pink colored emission (Figure 3). We have previously observed red-shifted emissions from aggregates of fluorinated phenoxy-**BsubPc**s[4b] though in the current case the long wavelength emissions are much more complicated in position and relative intensity. We are currently investigating the source of this observation. In devices whereby the **BsubPc** is functioning as a *p*-type material, an additional emission peak at 385 nm was observed as a result of EL emission from the TPBi layer. This could be eliminated by optimizing the thickness of each layer such that charges recombine within the desired **BsubPc** layer exclusively. The OLED emissions were plotted in CIE color space (Figure 8). The emission from devices containing compound **2** appears pink/purple, whereas those with compound **3** appear red/orange. Slight differences were observed when these compounds when functioning as either n-type or p-type.

CONCLUSIONS

In summation, we have shown that an additional nucleophile − phthalimide − can displace the halide of Cl-**BsubPc** thus producing a new class of **BsubPc** derivatives, phthalimido-boronsubphthalocyanines (Phth-**BsubPc**s), of which compounds **2** and **3** are representative examples. Phth-**BsubPcs** maintain the characteristically high quantum yield for photoluminescence (Φ) and extinction coefficient (ε) of known **BsubPc** derivatives. We have outlined an arrangement of the molecular orbitals of each derivative in the solid state through an examination of the extended crystallographic structure combined with calculations at the density functional theory level. Unlike other **BsubPc** derivatives, Phth-**BsubPcs** form both stable radical cations and radical anions under electrochemical conditions and we have shown this bipolar nature extends to their ability to act as both n-type and p-type charge carriers (and emitters) in OLEDs.

EXPERIMENTAL SECTION

Methods and Materials. All solvents were purchased from Caledon Laboratories Ltd. (Caledon, Ontario, Canada) and used as received unless stated otherwise. Phthalimide (99+%) was obtained from Sigma Aldrich and tetrachlorophthalimide was obtained from Eastbound Technologies Inc. and used as received. All nuclear magnetic resonance (NMR) spectra were acquired on a Varian Mercury 400 MHz system in deuterated chloroform ($CDCl_3$) purchased from Cambridge Isotope Laboratories which was used as received. All ^{1}H NMR spectra where referenced to an internal standard of 0.05% TMS. All X-ray crystallographic data was collected using computer-controlled KappaCCD system and an Oxford Cryostream variable temperature apparatus. Ring centroid proximities were calculated/measured by using Mercury version 2.3. All ultraviolet−visible (UV−vis) spectroscopy was performed using PerkinElmer Lambda 25 in a PerkinElmer quartz cuvette with a 10 mm path length for solution phase samples and on polished quartz wafers supplied by Ted Pella for thin film samples. Photoluminescence spectra were collected using a Perkin-Elmer LS 55. High-pressure liquid chromatography (HPLC) analysis was conducted using a Waters 2695 separation module with a Waters 2998 photodiode array and a Waters 4.6 mm ×100 mm SunFire C_{18} 3.5 μm column. HPLC grade acetonitrile (ACN) was eluted at 0.6 mL/min during operation. Cyclic voltammetry was performed with a Bioanalytical Systems C3 electrochemical workstation. The working electrode was a 1 mm platinum disk with a platinum wire used as a counter electrode. The reference electrode was Ag/AgCl saturated salt solution. All electrochemistry was done in spec-grade dichloromethane with tetrabutylammonium hexafluorophosphate (Bu_4NPF_6) as electrolyte which was purged with Argon at room temperature prior to use. Three cycles from +1.6 V to −1.6 V were measured for each compound at a scan rate of 100 mV/s. Decamethylferrocene was used as an internal reference. The half-wave reduction potential ($E_{1/2,red}$) of decamethylferrocene was previously measured to be −0.012 V vs Ag/AgCl.[28] Mass spectrometry was performed on a Waters GC time-of-flight mass spectrometer with an electron ionization probe and accurate mass determination. Carbon hydrogen nitrogen elemental analysis was performed using a Perkin-Elmer 2400 Series II CHNS Analyzer. HOMO and LUMO distributions were illustrated on structures geometrically optimized using the density functional theory (DFT) method with the Beck-Lee−Yang−Parr (B3LYP) exchange-correlation and the 6-31G* basis set as implemented in SPARTAN '06.

Device Preparation. Devices were prepared on a piece of ITO patterned glass (10 ohms/square). The glass patterned ITO substrate was cleaned with a standard regime of sonication in Alconox, acetone, and methanol, followed by a 15 min UV ozone treatment. Device layers were deposited by physical vapor deposition at a vacuum of $\sim 1 \times 10^{-8}$ Torr. The organic compounds and metals were deposited in separate chambers. Vacuum was maintained between each layer deposition of by way of a central distribution chamber. Top contact aluminum was deposited using a mask with strips 2 mm thick, resulting in device operating areas of 2 mm^2 and a minimum of four devices per structure. 1,3,5-Tris(N-phenylbenzimidazole-2-yl)benzene (TPBi) was purchased from Luminescence Technology Corp. and used as-received. *N,N′*-Bis(1-naphthyl)-*N,N′*-diphenyl-1,1′-biphenyl-4,4′-diamine (NPB) was purchased from Norel Optronics Inc. and used as received. LiF (99.99%) and MoO_3 (99.99%) were purchased from Sigma-Aldrich and were degassed in a high vacuum prior to use.

Chloro-boronsubphthalocyanine (1). Synthesized as previously reported.[23b]

Phthalimido-boronsubphthalocyanine (2). Cl-**BsubPc** (1.0 g, 2.3×10^{-3} mol) was combined with phthalimide (1.7 g, 1.2×10^{-2} mol) and dichlorobenzene (20 mL) in a 100 mL rounded bottom flask fitted with a condenser and held under a constant pressure of argon gas. The contents were heated at reflux (~180 °C) for 100 h. The solvent was removed by rotary evaporation yielding 3.24 g of crude product. 2.06 g of the crude was next train sublimated at 420 °C to remove all impurities resulting in 0.2 g of product (25% yield, 99.9% pure by HPLC and ^{1}H NMR). ^{1}H NMR (400 MHz, $CDCl_3$, Me_4Si): δ 7.19 to 7.21 (2H, q), 7.30 to 7.33 (2H, q), 7.92 to 7.94 (6H, q), 8.91 to 8.93 (6H, q). Anal. Calcd for $C_{32}H_{12}BCl_4N_7O_2$: C, 71.00; H, 2.98; N, 18.11. Found: C, 70.75; H, 3.28; N, 18.18. HRMS (positive) exact mass calcd for $C_{32}H_{16}BN_7O_2$, 541.1459; found, 541.1453. UV−$vis_{toluene}$ (log ε): 569 nm (4.84), 552 nm (4.54, shoulder), 308 nm (4.54). Crystals of suitable quantity for X-ray diffraction were grown by sublimation and slow vapor diffusion of heptane into chloroform.

Tetrachlorophthalimido-boronsubphthalocyanine (3). Cl-**BsubPc** (0.5 g, 1.2×10^{-3} mol) was combined with tetrachlorophthalimide (1.65 g, 5.8×10^{-3} mol) and dichlorobenzene (10 mL) in a 25 mL rounded bottom flask fitted with a condenser and held under a constant pressure of argon gas. The contents were heated at reflux (~180 °C) for 90 h. The completion of the reaction was confirmed by HPLC (absence of Cl-**BsubPc**) the reaction was let to cool to room temperature. The solvent was removed by rotary evaporation yielding a crude mass of 2.16 g. Next, 1.06 g of the crude product was purified by train sublimation at 460 °C yielding a mass of 0.094 g (yield 24%, 99.9% pure by HPLC and ^{1}H NMR). ^{1}H NMR (400 MHz, $CDCl_3$, Me_4Si): δ 7.92−7.95 (6H, m), 8.90−8.92 (6H, m). Anal. Calcd for $C_{32}H_{12}BCl_4N_7O_2$: C, 56.60; H, 1.78; N, 14.44. Found: C, 56.58; H, 1.91; N, 14.38. HRMS (positive) exact mass calcd for $C_{32}H_{12}BCl_4N_7O_2$, 676.9900; found, 676.9896. UV−$vis_{toluene}$ (log ε): 571 nm (4.72), 553 nm (4.50, shoulder), 305 nm (4.54). Crystals of suitable quantity for X-ray diffraction were grown by sublimation and slow vapor diffusion of heptane into chloroform.

***μ*-oxo-boronsubphthalocyanine Dimer (4).** Formed as a byproduct, because of trace amounts of H_2O present in the reaction vessel, and isolated by sublimation, as the large molecular weight of the dimer ensured a high sublimation point and did not sublimate (under the same conditions required to sublimate the phthalimido-**BsubPc**s) while the phthalimido-**BsubPc** and all other impurities were removed by sublimation. ^{1}H NMR (400 MHz, $CDCl_3$, Me_4Si): δ 7.76 to 7.78 (12H, m), 8.59 to 8.62 (12H, m). HRMS (positive) exact mass calcd for $C_{48}H_{24}B_2N_{12}O$, 806.2382; found, 806.2369. UV−vis (see Figure S7 in the Supporting Information).

■ ASSOCIATED CONTENT

Supporting Information. Complete experimental methods, spectroscopy data, crystallographic data for compounds **2** and **3**, computational details, and device performance details. This material is available free of charge via the Internet at http://pubs.acs.org.

■ AUTHOR INFORMATION

Corresponding Author
*E-mail: tim.bender@utoronto.ca.

■ ACKNOWLEDGMENT

We acknowledged the financial support from the National Sciences and Engineering Research Council (NSERC) for providing support in the form of a Discovery Grant (T.P.B., Z.H.L.), a Canada Graduate Scholarship (G.E.M., J.S.C.), and a Vanier Scholarship (M.G.H.).

■ REFERENCES

(1) Meller, A.; Ossko, A. *Monatsh. Chem.* **1972**, *103*, 150–155.

(2) (a) Mutolo, K. L.; Mayo, E. I.; Rand, B. P.; Forrest, S. R.; Thompson, M. E. *J. Am. Chem. Soc.* **2006**, *128*, 8108–8109. (b) Gommans, H.; Cheyns, D.; Aernouts, T.; Girotto, C.; Poortmans, J.; Heremans, P. *Adv. Funct. Mater.* **2007**, *17*, 2653–2658. (c) Gommans, H.; Aernouts, T.; Verreet, B.; Heremans, P.; Medina, A.; Claessens, C. G.; Torres, T. *Adv. Funct. Mater.* **2009**, *19*, 3435–3439. (d) Kumar, H.; Kumar, P.; Bhardwaj, R.; Sharma, G. D.; Chand, S.; Jain, S. C.; Kumar, V. *J. Phys. D: Appl. Phys.* **2009**, *42*, 015103. (e) Ma, B.; Woo, C. H.; Miyamoto, Y.; Frechet, J. M. J. *Chem. Mater.* **2009**, *21*, 1413–1417. (f) Klaus, D.; Knecht, R.; Dragässer, A.; Keil, C.; Schlettwein, D. *Phys. Status Solidi A* **2009**, *206* (12), 2723–2730. (g) Ma, B.; Miyamoto, Y.; Woo, C. H.; Fréchet, J. M. J.; Zhang, F.; Liu, Y. *Proc. SPIE* **2009**, *7416*, 74161E–1.

(3) (a) Xu, S.; Chen, K.; Tian, H. *J. Mater. Chem.* **2005**, *15* (27−28), 2676–2680. (b) Yang, Li, Y.; Xu, S.; Li, X.; Chen, K.; Tian, H. *Chem. Lett.* **2007**, *36* (5), 664–665. (c) Palomares, E.; Martínez-Díaz, M. V.; Torres, T.; Coronado, E. *Adv. Funct. Mater.* **2006**, *16*, 1166–1170. (d) Ros-Lis, J. V.; Martinez-Manez, R.; Soto, J. *Chem. Commun.* **2005**, 52605260.

(4) (a) Morse, G. E.; Helander, M. G.; Maka, J. F.; Lu, Z. H.; Bender, T. P. *ACS Appl. Mater. Interfaces* **2010**, *2* (7), 1934–1944. (b) Helander, M. G.; Morse, G. E.; Qiu, J.; Castrucci, J. S.; Bender, T. P.; Lu, Z. H. *ACS Appl. Mater. Interfaces* **2010**, *2* (11), 3147–3152. (c) Chen, Y. H.; Chang, Y. J.; Lee, G. R.; Chang, J. H.; Wu, I. W.; Fang, J. H.; Hsu, S. H.; Liu, S. W.; Wu, C. I.; Pi, T. W. *Org. Electron.* **2010**, *11*, 445–449. (d) Chen, Y. H.; Chang, J. H.; Lee, G. R.; Wu, I. W.; Fang, J. H.; Wu, C. I. *Appl. Phys. Lett.* **2009**, *95*, 133302. (e) Díaz, D. D.; Bolink, H. J.; Cappelli, L.; Claessens, C. G.; Coronado, E.; Torres, T. *Tetrahedron Lett.* **2007**, *48*, 4657–4660.

(5) (a) Yasuda, T.; Tsutsui, T. *Mol. Cryst. Liq. Cryst.* **2007**, *462*, 3–9. (b) Renshaw, K. C.; Xu, X.; Forrest, S. R. *Org. Electron.* **2010**, *11*, 175–178.

(6) (a) Claessens, C. G.; Torres, T. *J. Am. Chem. Soc.* **2002**, *124*, 14522–14523. (b) Claessens, C. G.; Torres, T. *Chem. Commun.* **2004**, 1298–1299. (c) Claessens, C. G.; Vincente-Arana, M. J.; Torres, T. *Chem. Commun.* **2008**, 6378–6380.

(7) (a) Claessens, C. G.; González-Rodríguez, D.; Iglesias, R. S.; Torres, T. *C. R. Chimie* **2006**, *9*, 1094–1099. (b) González-Rodríguez, D.; Carbonell, E.; Guldi, D. M.; Torres, T. *Angew. Chem., Int. Ed.* **2009**, *48*, 1–6.

(8) Xu, H.; Ermilov, E. A.; Roder, B.; Ng, D. K. P. *Phys. Chem. Chem. Phys.* **2010**, *12*, 7366–7370.

(9) (a) Xu, H.; Jiang, X.-J.; Chan, E. Y. M.; Fong, W.-P.; Ng, D. K. P. *Org. Biomol. Chem.* **2007**, *5*, 3987–3992. (b) Sharman, W. M.; van Lier, J. E. *Bioconjugate Chem.* **2005**, *16* (5), 1166–1175.

(10) Adachi, K.; Chayama, K.; Watarai, H. *Anal. Chem.* **2006**, *78*, 6840–6846.

(11) Claessens, C. G.; González-Rodríguez, D.; del Rey, B.; Torres, T.; Mark, G.; Schuchmann, H. P.; von Sonntag, C.; MacDonald, J. G.; Nohr, R. S. G. *Eur. J. Org. Chem.* **2003**, *14*, 2547–2551.

(12) (a) Kasuga, K.; Idehara, T.; Handa, M.; Ueda, Y.; Fujiwara, T.; Isa, K. *Bull. Chem. Soc. Jpn.* **1996**, *69*, 2559–2563. (b) Engel, M. K.; Yao, J.; Maki, H.; Takeuchi, H.; Yonehara, H.; Pac, C. *Kawamura Rikagaku Kenkyusho Hokoku* **1997**, 53–65.

(13) (a) Potz, R.; Goldner, M.; Huckstadt, H.; Cornelissen, U.; Tutass, A.; Homborg, H. *Z. Anorg. Allg. Chem.* **2000**, *626*, 588–596. (b) Eckert, A. K.; Rodriguez-Morgade, M. S.; Torres, T. *Chem. Commun.* **2007**, 4104–4106.

(14) (a) Del Rey, B; Martinez-Diaz, M. V.; Barbera, J.; Torres, T. *J. Porphyrins Phthalocyanines* **2000**, *4*, 569–573. (b) Geyer, M.; Plenzig, F.; Rauschnabel, J.; Hanack, M.; del Rey, B.; Sastre, A.; Torres, T. *Synthesis* **1996**, 1139–1151. (c) Zyskowski, C. D.; Kennedy, V. O. *J. Porphyrins Phthalocyanines* **2000**, *4*, 707–712.

(15) (a) Camerel, F.; Ulrich, G.; Retailleau, P.; Ziessel, R. *Angew. Chem., Int. Ed.* **2008**, *47*, 8876–8880. (b) Ziessel, R.; Ulrich, G.; Elliott, K. J.; Harriman, A. *Chem.—Eur. J.* **2009**, *15*, 4980–4984. (c) Mauldin, C. E.; Piliego, C.; Poulsen, D.; Unruh, D. A.; Woo, C.; Ma, B.; Mynar, J. L.; Fréchet, M. J. *ACS Appl. Mater. Interfaces* **2010**, *2* (10), 2833–2838.

(16) Guilleme, J.; González-Rodríguez, D.; Torres, T. *Angew. Chem., Int. Ed.*, **2011**, ASAP, DOI 10.1002/anie.201007240.

(17) More recently we have prepared compounds **2** and **3** starting from Br-**BsubPc**. Complete conversion to compounds **2** and **3** occurred within 4.5 h under otherwise identical conditions to that reported in the experimental section. Despite the shorter reaction time, between 10 and 13% of μ-oxo-(**BsubPc**)$_2$ (compound **4**) was still produced. All compounds and their respective properties reported herein are, however, derived from Cl-**BsubPc**.

(18) Kobayashi, N.; Ishizaki, T.; Ishii, K.; Konami, H. *J. Am. Chem. Soc.* **1999**, *121*, 9096.

(19) Gonzalez-Rodriguez, D.; Torres, T.; Guldi, D. M.; Rivera, J.; Herranz, M. A. A.; Echegoyen, L. *J. Am. Chem. Soc.* **2004**, *126*, 6301–6313.

(20) Anthony, J. E.; Brooks, J. S.; Eaton, D. L.; Parkin, S. R. *J. Am. Chem. Soc.* **2001**, *123*, 9482–9483.

(21) (a) Troisi, A.; Orlandi, G.; Anthony, J. E. *Chem. Mater.* **2005**, *17*, 5024–5031. (b) Coropceanu, V.; Cornil, J.; da Silva Filho, D. A.; Olivier, Y.; Silbey, R.; Brédas, J. L. *Chem. Rev.* **2007**, *107*, 926–952. (c) Kazmaier, P. M.; Hoffmann, R. *J. Am. Chem. Soc.* **1994**, *116*, 9684–9691. (d) Gregg, B. A.; Kose, M. E. *Chem. Mater.* **2008**, *20*, 5235–5239.

(22) For a discussion on terminology used for the description of the **BsubPc** molecular structure and its faces see refs 4a and 12b.

(23) (a) Paton, A. S.; Morse, G. E.; Lough, A. J.; Bender, T. P. *CrystEngComm.* **2011**, *13*, 914–919. (b) Morse, G. E.; Paton, A. S.; Lough, A. J.; Bender, T. P. *Dalton Trans.* **2010**, *39*, 3915–3922.

(24) (a) Claessens, C. G.; Torres, T. *Angew. Chem., Int. Ed.* **2002**, *41* (14), 2561–2565. (b) Paton, A. S.; Morse, G. E.; Maka, J. F.; Lough, A. J.; Bender, T. P. *Acta Crystallogr., Sect. E* **2010**, *66*, o3059.

(25) Morse, G. E.; Helander, M. G.; Stanwick, J.; Sauks, J. M.; Paton, A. S.; Lu, Z. H.; Bender, T. P. *J. Phys. Chem. C* **2011**, *115*, 11709–11718.

(26) D'Andrade, B. W.; Datta, S.; Forrest, S. R.; Djurovich, P.; Polikarpov, E.; Thompson, M. E. *Org. Electron.* **2005**, *6*, 11–20.

(27) Van Slyke, S. A.; Chen, C. H.; Tang, C. W. *Appl. Phys. Lett.* **1996**, *15*, 2160–2162.

(28) (a) Bender, T. P.; Graham, J. F.; Duff, J. M. *Chem. Mater.* **2001**, *13*, 4105–4111. (b) Noviandri, I.; Brown, K. N.; Fleming, D. S.; Gulyas, P. T.; Lay, P. A.; Masters, A. F.; Phillips, L. *J. Phys. Chem. B* **1999**, *103*, 6713–6722.